

Practical 12.5-Gb/s, 12.5-GHz spaced ultra-dense WDM PON

H. K. Shim, Hoon Kim, and Y. C. Chung*

Department of Electrical Engineering, Korea Advanced Institute of Science and Technology (KAIST) 291 Daehak-ro,
Yuseong-gu, Daejeon 305-701, South Korea
ychung@ee.kaist.ac.kr

Abstract: We report a practical 12.5-Gb/s, 12.5-GHz-spaced ultra-dense wavelength-division-multiplexed passive optical network (UD-WDM PON). For the cost-effectiveness, we implement the downstream links by using electro-absorption modulated lasers (EMLs) in the 4-level pulse amplitude modulation (4PAM) format and PIN receivers, and the upstream links by using reflective semiconductor optical amplifiers (RSOAs) modulated in the quadrature phase-shift-keying (QPSK) format and low-cost self-homodyne receivers. To further enhance its cost-effectiveness, we also utilize an optical frequency comb generator, instead of a large number of wavelength-selected lasers, to provide the seed light for these colorless RSOAs. We optimize the operating conditions of the EMLs and RSOAs to maximize the power margins in the presence of the crosstalk arising from closely spaced neighboring channels and the inter-symbol interference (ISI) caused by the narrow passband of the cascaded arrayed-waveguide gratings (AWGs) as well as the limited modulation bandwidths of RSOAs. The experimental results show that we can secure the power margins of >2.5 dB for both upstream and downstream links of the proposed UD-WDM PON.

©2014 Optical Society of America

OCIS codes: (060.2360) Fiber optics links and subsystems; (060.1660) Coherent communications.

References and links

1. H. Rohde, S. Smolorz, E. Gottwald, and K. Kloppe, "Next generation optical access: 1 Gbit/s for everyone," in *Proc. of European Conference on Optical Communication 2009*, paper 10.5.5.
2. S. Smolorz, E. Gottwald, H. Rohde, D. Smith, and A. Poustie, "Demonstration of a coherent UDWDM-PON with real-time processing," in *Proc. of Optical Fiber Communication 2011*, paper PDPD4.
3. D. Lavery, M. Ionescu, S. Makovejs, E. Torrenco, and S. J. Savory, "A long-reach ultra-dense 10 Gbit/s WDM-PON using a digital coherent receiver," *Opt. Express* **18**(25), 25855–25860 (2010).
4. Z. Dong, X. Li, J. Yu, Z. Cao, and N. Chi, "8 × 9.95-Gb/s ultra-dense WDM-PON on a 12.5-GHz grid with digital pre-equalization," *IEEE Photon. Technol. Lett.* **25**(2), 194–197 (2013).
5. J. D. Reis, A. Shahpari, R. Ferreira, S. Ziaie, D. M. Neves, M. Lima, and A. Teixeira, "Terabit+ (192×10 Gb/s) Nyquist shaped UDWDM coherent PON with upstream and downstream over a 12.8 nm band," *J. Lightwave Technol.* **32**(4), 729–735 (2014).
6. Z. Dong, J. Yu, H. C. Chien, N. Chi, L. Chen, and G. K. Chang, "Ultra-dense WDM-PON delivering carrier-centralized Nyquist-WDM uplink with digital coherent detection," *Opt. Express* **19**(12), 11100–11105 (2011).
7. R. S. Luis, A. Shahpari, J. D. Reis, R. Ferreira, Z. Vujcic, B. J. Puttnam, J. M. D. Mendinueta, M. Lima, M. Nakamura, Y. Kamio, N. Wada, and A. Teixeira, "Ultra high capacity self-homodyne PON with simplified ONU and burst-mode upstream," *IEEE Photon. Technol. Lett.* **26**(7), 686–689 (2014).
8. Y. C. Chung, "Recent advancement in WDM PON technology," in *Proc. of European Conference on Optical Communication 2011*, paper Th.11.C.4.
9. S. P. Jung, Y. Takushima, and Y. C. Chung, "Generation of 5-Gbps QPSK signal using directly modulated RSOA for 100-km coherent WDM PON," in *Proc. of Optical Fiber Communication 2011*, paper OTuB3.
10. M. Fujiwara, J. Kani, H. Suzuki, K. Araya, and M. Teshima, "Flattened optical multicarrier generation of 12.5 GHz spaced 256 channels based on sinusoidal amplitude and phase hybrid modulation," *Electron. Lett.* **37**(15), 967–968 (2001).
11. S. J. Park, Y. B. Choi, S. P. Jung, K. Y. Cho, Y. Takushima, and Y. C. Chung, "Hybrid WDM/TDMA-PON using self-homodyne and differential coding," *IEEE Photon. Technol. Lett.* **21**(7), 465–467 (2009).

12. K. Y. Cho, K. Tanaka, T. Sano, S. P. Jung, J. H. Chang, Y. Takushima, A. Agata, Y. Horiuchi, M. Suzuki, and Y. C. Chung, "Long-reach coherent WDM PON employing self-polarization-stabilization technique," *J. Lightwave Technol.* **29**(4), 456–462 (2011).
13. J. Zhou, C. Yu, and H. Kim, "1.5- μ m, 10-Gbps 4-PAM VCSEL transmission for optical access networks," in *Proc. of International Conference on Optical Internet 2014*, paper FA2–3.
14. M. Funabashi, H. Nasu, T. Mukaiharu, T. Nomura, and A. Kasukawa, "Recent advances in DFB lasers for ultradense WDM applications," *IEEE J. Sel. Top. Quantum Electron.* **10**(2), 312–318 (2004).
15. D. K. Jung, S. K. Shin, H. G. Woo, and Y. C. Chung, "Wavelength-tracking technique for spectrum-sliced WDM passive optical network," *IEEE Photon. Technol. Lett.* **12**(3), 338–340 (2000).
16. G. Agrawal, *Fiber-optic communication systems*, 3rd Ed., (Wiley, 2002).
17. K. Inoue, "Four-wave mixing in an optical fiber in the zero-dispersion wavelength region," *J. Lightwave Technol.* **10**(11), 1553–1561 (1992).
18. I. Kaminow and T. Koch, *Optical fiber telecommunications IIIA*, (Academic, 1997).
19. M. Eiselt, "Limits on WDM systems due to four-wave mixing: a statistical approach," *J. Lightwave Technol.* **17**(11), 2261–2267 (1999).
20. H. Takahashi, K. Oda, and H. Toba, "Impact of crosstalk in an arrayed-waveguide multiplexer on N \times N optical interconnection," *J. Lightwave Technol.* **14**(6), 1097–1105 (1996).
21. R. Wu, V. R. Supradeepa, C. M. Long, D. E. Leaird, and A. M. Weiner, "Generation of very flat optical frequency combs from continuous-wave lasers using cascaded intensity and phase modulators driven by tailored radio frequency waveforms," *Opt. Lett.* **35**(19), 3234–3236 (2010).
22. K. Y. Cho, U. H. Hong, S. P. Jung, Y. Takushima, A. Agata, T. Sano, Y. Horiuchi, M. Suzuki, and Y. C. Chung, "Long-reach 10-Gb/s RSOA-based WDM PON employing QPSK signal and coherent receiver," *Opt. Express* **20**(14), 15353–15358 (2012).
23. K. H. Lee, K.-H. Park, and W. Y. Choi, "Measurement of the carrier lifetime and linewidth enhancement factor of semiconductor optical amplifiers using their optical modulation responses," *Opt. Eng.* **43**(11), 2715–2718 (2004).
24. K. Y. Cho, Y. Takushima, and Y. C. Chung, "Enhanced operating range of WDM PON implemented by using uncooled RSOAs," *IEEE Photon. Technol. Lett.* **20**(18), 1536–1538 (2008).
25. M. Fujiwara, J. Kani, H. Suzuki, and K. Iwatsuki, "Impact of backreflection on upstream transmission in WDM single-fiber loopback access networks," *J. Lightwave Technol.* **24**(2), 740–746 (2006).

1. Introduction

Recently, there have been growing interests in ultra-dense wavelength-division-multiplexed passive optical networks (UD-WDM PONs) to provide broadband services to a large number of subscribers cost-effectively [1–7]. For example, it has been proposed to develop an UD-WDM PON capable of providing 1-Gb/s service to ~1000 subscribers by using tunable lasers and digital coherent receivers [1, 2]. There also have been some efforts to develop high-speed (≥ 10 Gb/s/channel) UD-WDM PONs for the use in future optical access networks [3–7]. These networks utilize the multi-level modulation format, digital coherent receivers, digital pre-equalization technique, and/or Nyquist pulse shaping to minimize the channel spacing and maximize the spectral efficiency. However, most of these networks may not be cost-effective enough for the practical deployment due to their use of the expensive I/Q modulators, tunable lasers, and digital coherent receivers similar to those used in long-haul networks. For the development of the cost-effective UD-WDM PONs, we believe that it is essential to implement the optical network units (ONUs) colorless, utilize the single-fiber bidirectional transmission, avoid the use of expensive external modulators, and minimize the use of optical amplifiers [8].

In this paper, we propose and demonstrate a cost-effective 12.5-GHz spaced UD-WDM PON operating at the per-wavelength speed of 12.5 Gb/s for both downstream and upstream links. The downstream signals are transmitted by using electro-absorption modulated lasers (EMLs) in the 4-level pulse amplitude modulation (4PAM) format and direct-detection PIN receivers, while the upstream signals are transmitted by utilizing reflective semiconductor optical amplifiers (RSOAs) directly modulated in the quadrature phase-shift keying (QPSK) format and inexpensive self-homodyne coherent receivers previously developed for the use in the access networks [9]. To further enhance the cost-effectiveness of the proposed UD-WDM PON system, an optical frequency comb generator is utilized to provide the seed light for these colorless RSOAs instead of a large number of tunable lasers or wavelength-selected distributed feedback (DFB) laser diodes [10]. To the best of our knowledge, this result

represents the first demonstration of the high-speed (>10 Gb/s) UD-WDM PON implemented by using inexpensive light sources such as EMLs and directly modulated RSOAs. To evaluate the possibility of realizing this potentially practical UD-WDM PON, we investigate the effects of narrow optical filtering and optical crosstalk on the performances of the 12.5-GHz-spaced, 12.5-Gb/s upstream and downstream signals generated by using these light sources.

2. Configuration of the proposed UD-WDM PON

Figure 1 shows the configuration of the proposed 12.5-GHz spaced UD-WDM PON capable of providing symmetric 12.5-Gb/s services to each subscriber. We assume that the upstream and downstream links of this network operate at two different wavelength bands. The downstream links are implemented by using EMLs modulated in the 4PAM format at the optical line terminal (OLT) and direct-detection receivers at the ONUs. These 4PAM signals, spaced at 12.5 GHz, are multiplexed by using an arrayed waveguide grating (AWG3) at the OLT, and transmitted through a 20-km long standard single-mode fiber (SSMF). The downstream signals are then detected by PIN receivers after being demultiplexed by AWG4 at the remote node (RN) and separated from the seed light by a wavelength-division multiplexer at the ONU.

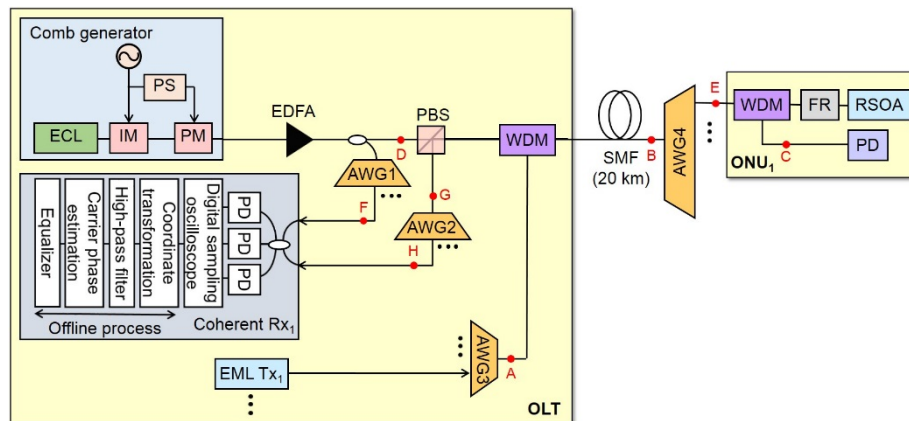


Fig. 1. Configuration of the proposed 12.5-Gb/s, 12.5-GHz spaced UD-WDM PON (Tx: transmitter; Rx: receiver; ECL: external-cavity laser; IM: intensity modulator; PM: phase modulator; PS: phase shifter; PBS: polarization-beam splitter; AWG: arrayed-waveguide grating; PD: photo-detector; EML: electro-absorption modulated laser; WDM: wavelength-division multiplexer; FR: Faraday rotator; RSOA: reflective semiconductor optical amplifier).

For the upstream transmission, we utilize colorless RSOAs modulated in the QPSK format at the ONUs and inexpensive self-homodyne coherent receivers at the OLT. When we directly modulate the injection current of an RSOA, both the amplitude and phase of its output signal vary with the modulation current since its gain and refractive index are dependent on the carrier density. Thus, we can utilize the RSOA as a phase modulator for the generation of the QPSK signal. For the use of RSOAs, however, it is necessary to provide the seed light to each ONU. For this purpose, instead of using a bank of tunable lasers or wavelength-selected DFB lasers at the OLT, we utilize an optical frequency comb generator composed of an intensity modulator and a phase modulator, as shown in Fig. 1. The 12.5-GHz-spaced optical comb signals are transmitted over the 20-km long SSMF, demultiplexed by AWG4, and sent to their corresponding ONUs for the use as the seed light. At each colorless ONU, this seed light is modulated in the QPSK format by directly modulating an RSOA with an electrical 4PAM signal and sent back to the OLT. The upstream signals are then detected by using the self-homodyne receivers implemented cost-effectively by using 3×3 couplers as 120° optical hybrids instead of using the expensive 90° optical hybrids (typically composed of four 2×2 couplers) [11]. These coherent receivers implemented by using 3×3 couplers outperform the

conventional coherent receivers based on 90° optical hybrids when the system's performance is limited by the receiver noises. This is because the splitting loss of the 3×3 coupler is 1.25 dB ($= 10 \cdot \log 4 - 10 \cdot \log 3$) lower than that of the 90° optical hybrid. The performance of the UD-WDM PON system is typically limited by the receiver noises when the crosstalk from neighboring channels is insignificant. A portion of the seed light is used as a local oscillator (LO) in these self-homodyne receivers. For example, we tap a portion of the generated comb signal at the OLT, demultiplex it by using AWG1, and send the demultiplexed comb to each self-homodyne receiver. There is no need to utilize the expensive polarization-diversity or polarization-tracking technique in these receivers since we stabilize the state-of-polarization (SOP) of the upstream signals by placing a Faraday rotator (FR) in front of each RSOA at the ONU [12].

3. Experimental results of the downstream links

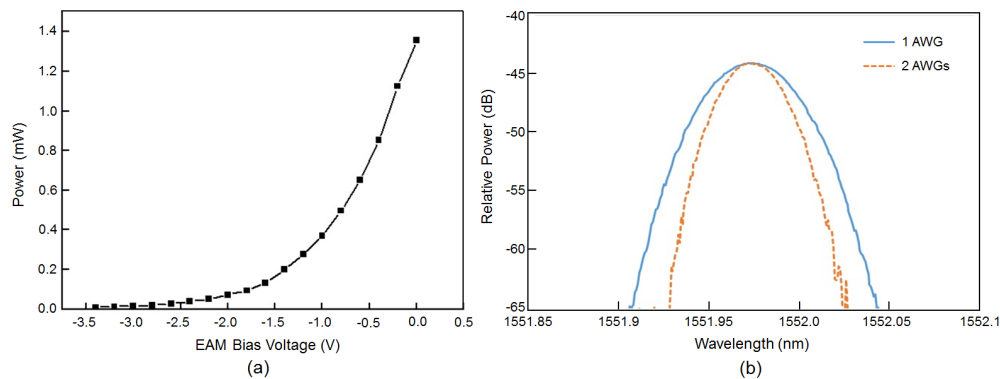


Fig. 2. (a) Measured transfer curve of the EML and (b) transmittance of the AWGs used in this experiment.

For a demonstration, we implemented the proposed UD-WDM PON shown in Fig. 1 by using two adjacent channels in each direction. The downstream links were implemented by using two EMLs operating at 1553.15 and 1553.25 nm, and modulated at the speed of 12.5 Gb/s in the 4PAM format. The operating temperatures of these 7-pin butterfly-packaged EMLs were controlled for the wavelength stabilization. Figure 2(a) shows the output power of the EML measured as a function of the bias voltage applied to the electro-absorption modulator (EAM) integrated within the EML. A nonlinear transfer curve was observed with respect to the bias voltage. Thus, to generate an equally spaced optical 4PAM signal by modulating the EML with an equally spaced 4-level electrical signal, it was necessary to utilize the linear portion of this curve. For this purpose, we set the bias voltage of the EAM to be -0.3 V. Under this condition, the chirp parameter was measured to be 0.36. The EML signals, modulated in the 4PAM format, were sent to the ONUs after passing through two AWGs (i.e., AWG3 and AWG4 in Fig. 1) and the 20-km long feeder fiber. In this experiment, we utilized Gaussian-shaped non-cyclic 1×24 AWGs having a channel spacing of 12.5 GHz. The insertion loss of these AWGs was ~ 5 dB. Figure 2(b) shows the transmittance of the AWGs. The 3-dB passband of the AWGs was measured to be ~ 6.8 GHz. However, when we cascaded two of these AWGs, it was reduced to ~ 4.8 GHz. At the ONU, the 12.5-Gb/s 4PAM downstream signals were detected by using PIN receivers and then sent to a digital sampling oscilloscope for the post-detection electronic equalization and bit-error rate (BER) measurement. A 7-tap feed-forward equalizer (FFE) followed by a 5-tap decision-feedback equalizer (DFE) was utilized for the compensation of the inter-symbol interference (ISI) caused by the narrow passband of the cascaded AWGs.

We first optimized the extinction ratio (ER) of the downstream signals in the back-to-back condition. In this measurement, we turned off the neighboring channel to exclude the effects

of crosstalk and measured the bit-error rate (BER) curves of an EML signal while varying its ER, as shown in Fig. 3. We also measured the BER curves with and without the AWGs (i.e., without AWG3 and AWG4) to estimate the effects of ISI. For the 4PAM signal, the ER was defined as the ratio between the highest and lowest intensity levels. As expected, in the absence of the cascaded AWGs, the receiver sensitivity ($@ \text{BER} = 10^{-3}$) of this 4PAM signal was improved as we increased the ER. For example, the receiver sensitivities of -15.4 , -17.0 , and -18.2 dBm were obtained when we set the ERs of this 4PAM signal to be 1.6, 2.6, and 3.5 dB, respectively. However, the maximum achievable ER was limited to be 3.5 dB due to the limited linear range of the EML's transfer curve used in this experiment. The power penalty of the 4PAM signal caused by the limited ER can be expressed as [13]

$$\text{Penalty} = 10 \cdot \log_{10}[(ER + 1)/(ER - 1)] \quad (\text{dB}) \quad (1)$$

The measured penalties agreed well with the calculated values by using this equation. For example, when we set the ER of this 12.5-Gb/s 4PAM signal to be 2.6 dB and 3.5 dB, the difference in their measured penalties was 1.2 dB, which was identical to the calculated value. The performances of these downstream signals could be deteriorated by the ISI when we installed two AWGs (i.e., AWG3 and AWG4) in place. However, due to the use of the 4PAM format as well as the small chirp parameter of the EML, the 20-dB spectral width of the modulated EML signal was measured to be only 5.3 GHz, which was comparable to the 3-dB bandwidth of the cascaded AWGs (i.e., ~ 4.8 GHz). Thus, the ISI penalties caused by these two AWGs were measured to be only 1.1~1.7 dB, as shown in Fig. 3. Due to the small chirp parameter, the spectral width of the modulated EML signal was maintained to be nearly constant regardless of the ER. As a result, the best receiver sensitivity of -17.0 dBm was achieved at the maximum ER of 3.5 dB.

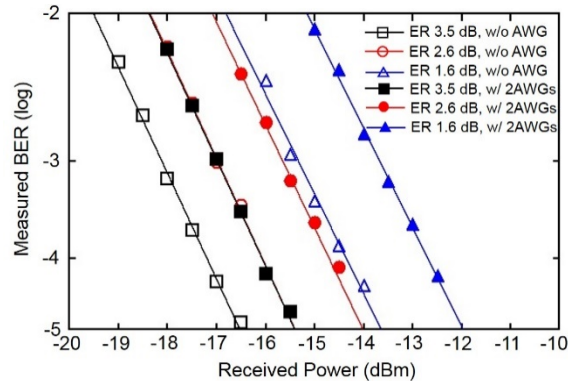


Fig. 3. BER curves of the 12.5-Gb/s downstream signal in the 4PAM format measured with and without the two AWGs on the link.

It should be noted that the small ISI-induced power penalties could be obtained only when the operating wavelength of the EML was precisely aligned to the center wavelengths of the AWGs. Figure 4 shows the measured power penalties as a function of the frequency offset between the EML and AWGs, while setting the ER of the 4PAM signal to be 3.5 dB. In this measurement, we adjusted the bias current of the EML to evaluate the effects of the frequency offset between the EML's operating wavelength and the center wavelength of the cascaded AWGs. The results showed that this frequency offset should be maintained within ± 1.0 GHz to maintain the ISI-induced power penalty to be < 0.5 dB. This requirement of the frequency offset is readily achievable by using either the commercially available wavelength lockers or the wavelength-tracking circuitries [14, 15].

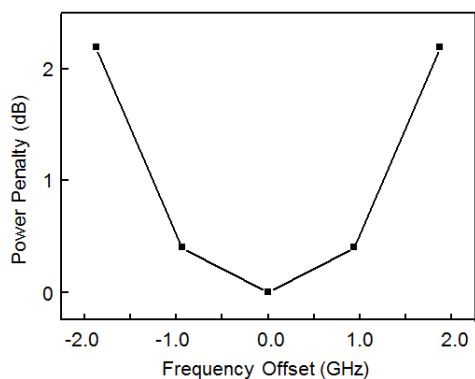


Fig. 4. Measured power penalties of the 12.5-Gb/s downstream 4PAM signals as a function of the frequency offset between the operating wavelength of EML and the center wavelength of the cascaded AWGs' passband.

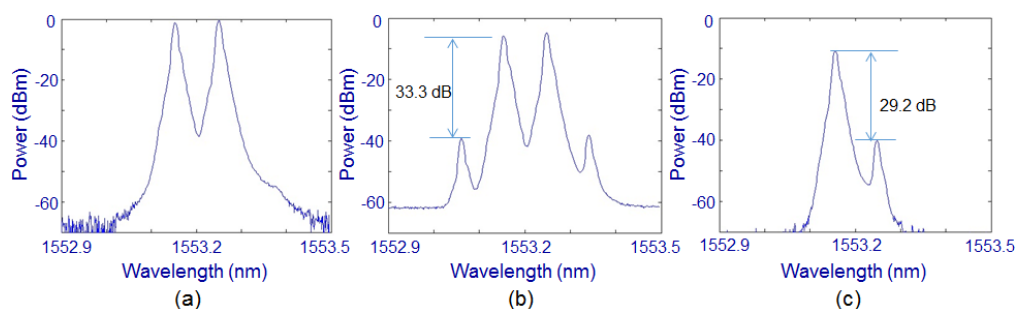


Fig. 5. Optical spectra of the downstream EML signals measured at (a) point A, (b) point B, and (c) point C in Fig. 1.

We also investigated the effects of the crosstalk arising from the neighboring channels. For this purpose, we utilized both EMLs operating at 1553.15 and 1553.25 nm. Figures 5(a), 5(b) and 5(c) show the optical spectra of the 12.5-Gb/s 4PAM signals measured at points A, B and C in Fig. 1, respectively. The optical power of each downstream signal was 6 dBm at the input of AWG3. The measured optical spectra showed that these two 12.5-GHz spaced EML signals could be well separated by using AWG4 at the RN. For example, the crosstalk component was measured to be -29.2 dB lower than the signals after the demultiplexer (i.e., AWG4), as shown in Fig. 5(c). Thus, the total linear crosstalk arising from two immediately neighboring channels was expected to be less than -26 dB (i.e., assuming that we launched another neighboring channel at 1553.05 nm). However, due to incoherent nature of the hetero-wavelength crosstalk, this would incur only 0.2-dB penalty [16]. On the other hand, due to the narrow channel spacing, small four-wave mixing (FWM) products were observed at around 1552.95 and 1553.35 nm, as shown in Fig. 5(b). The optical power ratio between the signals and FWM products was measured to be -33.3 dB, which agreed well with the theoretically calculated value of -32.0 dB [17]. In this experiment, we intentionally aligned the polarization states of two signals to maximize the FWM products shown in Fig. 5(b). It is well known that, in the N -channel WDM system, the total number of the FWM products is $(N^3 - N^2)/2$ [18]. However, in the WDM systems implemented by using SSMF, 4~6 closest neighboring channels contribute to the FWM penalty [19]. Thus, we estimated the FWM penalty occurred in the proposed UD-WDM PON by considering six neighboring channels. For the worst-case analysis, we also assumed that all six channels had same SOP. Thus, 11 non-degenerate and 2 degenerate FWM products could be fallen on the center channel. In this case, the total optical power of the FWM products was calculated to be 21 dB lower than the signal power. The power penalty induced by this nonlinear crosstalk was estimated to be <0.4

dB (@ BER = 10^{-3}) [20]. Thus, the FWM would not cause any serious problem in the proposed UD-WDM PON.

Figure 6 shows the BER curves of the 12.5-Gb/s 4PAM downstream signals measured with and without the neighboring channel. The receiver sensitivities (@ BER = 10^{-3}) of these downstream signals were measured to be -17.0 dBm in the back-to-back condition and -16.8 dBm after the transmission over the 20 km of SSMF. The power penalties caused by the linear crosstalk and fiber dispersion were measured to be <0.1 dB and ~ 0.2 dB, respectively. Thus, we estimated that the power budgets of the downstream links in the proposed UD-WDM PON would be ~ 22.4 dB (considering that the output power of the EML was 6 dBm and the FWM penalty was <0.4 dB). The total insertion loss of various optical components used in the downstream links including two AWGs (2×5 dB), two wavelength-division multiplexers (2×1 dB), and 20-km long feeder fiber (0.25 dB/km $\times 20$ km) was ~ 17 dB. Thus, this power budget would be sufficient to support the transmission of 12.5-GHz spaced, 12.5-Gb/s downstream signals in the proposed UD-WDM PON without using any optical amplifiers.

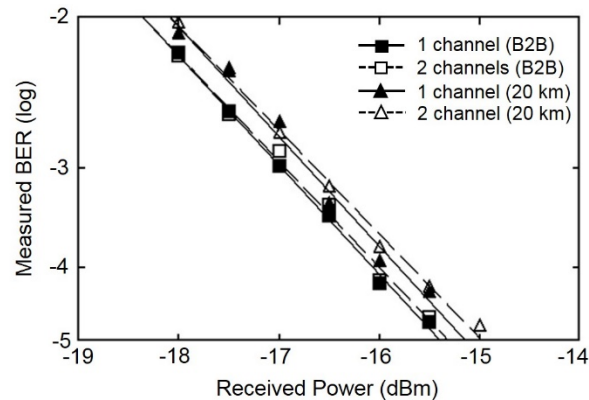


Fig. 6. BER curves of the 12.5-Gb/s downstream signals generated by using EMLs.

4. Experimental results of the upstream links

For the demonstration of the upstream links, we utilized two RSOAs directly modulated in the QPSK format at the speed of 12.5 Gb/s [9]. The seed light was provided to these colorless RSOAs by using an optical comb generator located at the OLT. For the generation of the 12.5-GHz spaced frequency comb, we injected the output of a tunable laser operating at 1552.16 nm into a set of intensity and phase modulators, as shown in Fig. 1. A 12.5-GHz sinusoidal wave was applied to both of these modulators and a phase shifter was used for their synchronization. In this comb generator, the maximum number of the generated comb lines was determined by the ratio between the V_{π} voltage of the phase modulator and the maximum amplitude of its driving signal. The V_{π} voltage of the phase modulator used in this comb generator was 3 V. By using this phase modulator together with an intensity modulator, we could generate up to 19 comb lines with a spectral flatness of 3 dB. However, if necessary, we could increase this number substantially by applying the outputs of additional lasers operating at different wavelengths into the same set of modulators [10]. Thus, by using this optical comb generator, we should be able to reduce the number of wavelength-selected lasers required for providing the seed light to every ONU by a factor of 19. Previously, it has been demonstrated that as many as 38 comb lines could be generated with excellent flatness by using one laser and a set of intensity and phase modulators [21]. Thus, it is expected that, by using such an optical comb generator and only 9 wavelength-selected lasers, it would be possible to provide the seed light for ~ 350 ONUs and cover the entire C-band.

The optical comb lines were demultiplexed by AWG4 after passing through the 20-km long feeder fiber and sent to each RSOA for the use as the seed light. The optical power of

this seed light was set to be larger than -9 dBm at the input of the RSOA since the modulation bandwidth of the RSOA slightly increased with the optical power of the seed light. Under this condition, the RSOA provided an optical gain of ~ 11 dB. The polarization-dependent gain of the RSOA was measured to be ~ 1 dB. We generated the 8B/10B-encoded 12.5-Gb/s upstream signals in the QPSK format by directly modulating the RSOAs. These signals were transmitted back to the OLT and detected by using the self-homodyne receivers. There was no need to utilize the polarization-diversity technique as we placed an FR in front of the RSOA at the ONU. The polarization fluctuations occurring in AWG1 and AWG2 were negligible throughout this experiment. We sampled the detected signals at 40 GSamples/s by using a digital sampling oscilloscope and applied the coordinate transformation to obtain I- and Q-components. The low-frequency components resulting from Rayleigh backscattering was eliminated simply by applying a high-pass filter having a cutoff frequency of 20 MHz. The performances of the upstream signals were not affected by this high-pass filtering due to the use of the 8B/10B line coding [22]. The carrier phase of the generated QPSK signal was estimated by using the M-th power algorithm. We utilized the electronic equalization technique based on the 16-tap feed-forward equalizer (FFE) and 10-tap distributed-feedback equalizer (DFE) to compensate for the limited modulation bandwidth of the RSOA before counting errors.

The modulation bandwidth of a typical RSOA is 1~3 GHz. Thus, when we generated the 12.5-Gb/s QPSK signal by modulating an RSOA with a 6.25-Gbaud 4-level electrical signal, this signal could seriously suffer from ISI due to its limited modulation bandwidth. To mitigate this problem, we attempted to maximize the modulation bandwidth of the RSOA by increasing its bias current [23,24]. For example, the modulation bandwidth of the RSOA used in this experiment was only 1.2 GHz at the bias current of 40 mA. However, we could increase it to 3.2 GHz by increasing the bias current to 80 mA. On the other hand, as we increased the bias current of the RSOA, its dynamic chirp was slightly reduced. As a result, it was necessary to increase the amplitude of the modulation current to achieve the maximum Euclidean distance between the adjacent symbols of the QPSK signal in the phasor diagram. Thus, for the rotation of the optical phase of the modulated signal by $3\pi/2$, we increased the peak-to-peak modulation current of the RSOA from 25 mA_{p-p} to 55 mA_{p-p} when we increased its bias current from 40 mA to 80 mA, respectively. Nevertheless, the spectral width of the modulated signal remained to be nearly constant.

Figure 7 shows the BER curves measured in the back-to-back condition while varying the bias current of the RSOA. We increased the bias current of the RSOA from 40 mA to 80 mA and adjusted its peak-to-peak modulation current to ensure the sufficient rotation of the optical phase for the generation of the QPSK signal. Accordingly, the peak-to-peak amplitude of the modulation current was increased from 25 mA_{p-p} to 55 mA_{p-p}. In the absence of the AWGs, the receiver sensitivities were improved as we increased the bias current of the RSOA. For example, the receiver sensitivities (@ BER = 10^{-3}) of the 12.5-Gb/s upstream QPSK signal were measured to be -32.8 dBm and -38.0 dBm at the bias currents of 40 mA and 80 mA, respectively. This was mainly due to the improved modulation bandwidth of the RSOA with the increased bias current. On the other hand, when we installed two AWGs in the link (i.e., AWG2 and AWG4 in Fig. 1), the receiver sensitivity was deteriorated by the ISI substantially. For example, the ISI penalties caused by the narrow passband of the cascaded AWGs were measured to be ~ 4 dB regardless of the bias current, as shown in Fig. 7. This was because the linewidth enhancement factor (LEF) of the RSOA was quite large (i.e., ~ 10). As a result, the spectral width of the QPSK signal generated by the RSOA was dominated by the phase modulation rather than intensity modulation. Thus, regardless of the bias current, the spectral width of the 12.5-Gb/s QPSK signal generated by using an RSOA could be estimated as

$$\Delta\nu = \frac{1}{2\pi} \frac{\Delta\phi}{\Delta t} \approx \frac{1}{2\pi} \frac{3\pi/2}{1/6.25 \text{ GHz}} = 4.7 \text{ GHz} \quad (2)$$

when the peak-to-peak amplitude of the modulation current was adjusted to rotate the optical phase of the QPSK signal by $3\pi/2$. In this equation, $\Delta\phi/\Delta t$ represents the change of the optical phase with respect to time. Thus, under this modulation condition, the effect of ISI on this QPSK signal was not dependent on the bias currents, as shown in Fig. 7. It should be noted that the upstream signals suffered much more than the downstream signals from the ISI induced by the cascaded AWGs. We attributed this to the fact that RSOAs had much larger LEF than EMLs. Nevertheless, due to the use of the coherent receivers for the upstream signals, we could still achieve the excellent receiver sensitivity of -33.8 dBm (when the bias current of the RSOA was set to be 80 mA).

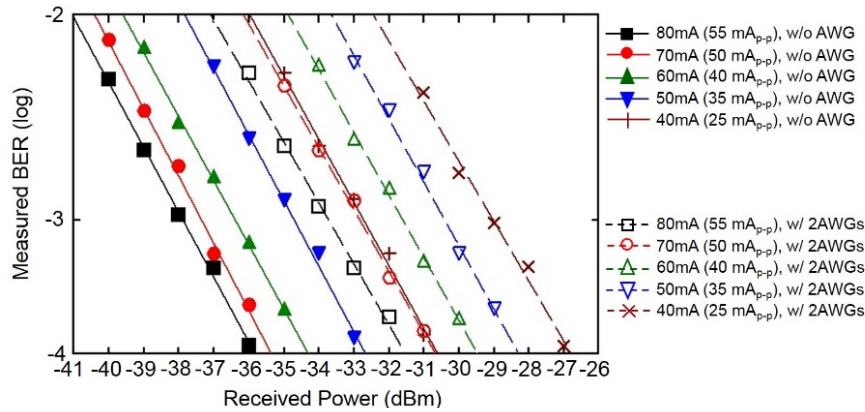


Fig. 7. Measured BER curves of the 12.5-Gb/s QPSK upstream signals in the back-to-back condition.

Figure 8(a) shows the optical spectrum of the frequency comb measured at the OLT (i.e., at point D in Fig. 1). We could obtain 19 comb lines spaced at 12.5 GHz within 3-dB spectral power variation. The optical power of each comb line was ~ 6 dBm at the output of the Erbium-doped fiber amplifier (EDFA). We sent two adjacent comb lines (at 1551.96 and 1552.06 nm) to their corresponding ONUs via AWG4. Figure 8(b) shows the optical spectrum of one of these comb lines measured at point E. The neighboring comb lines were suppressed by >30 dB at the input of the ONU. The optical power of the comb line (i.e., seed light) incident on the RSOA was -9 dBm. Figure 8(c) shows the optical spectrum of the comb line used as an LO (measured at point F). The optical power of the LO light incident on the coherent receiver was -0.6 dBm. Figures 8(d) and 8(e) show the optical spectra of the upstream signals measured before and after the demultiplexer at the OLT (i.e., at points G and H), respectively. These figures show that the crosstalk components caused by the neighboring channels were suppressed by >40 dB by AWG2. Thus, the power penalties caused by these small crosstalk components would be negligible even when the received powers of two neighboring channels differ by 10 dB [16].

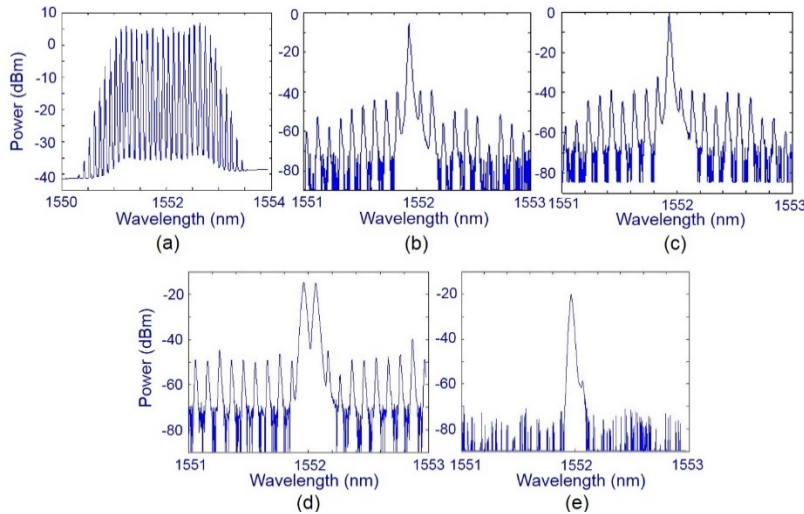


Fig. 8. Optical spectra of the (a) the generated optical frequency comb measured at point D, (b) one of the demultiplexed comb lines (used as the seed light) measured at point E, (c) one of the demultiplexed comb lines (used as an LO) measured at point F, (d) two upstream signals in the QPSK format measured at point G, and (e) the demultiplexed upstream signal measured at point H in Fig. 1.

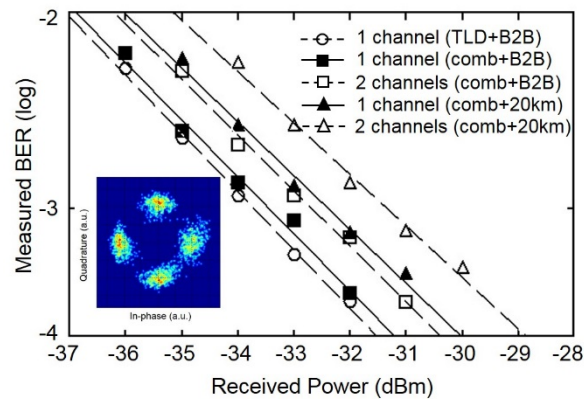


Fig. 9. BER curves of the 12.5-Gb/s upstream QPSK signals measured by using either tunable lasers or a comb generator for the seed light. The inset shows the constellation of the upstream signal after 20-km transmission (@ received power = -30 dBm). TLD: tunable laser diode.

Figure 9 shows the BER curves of the 12.5-Gb/s upstream QPSK signals measured after the transmission over the 20-km long feeder fiber with and without the neighboring channel. For comparison, we also plotted the BER curves measured under the same conditions without the feeder fiber in this figure. The results showed that the crosstalk penalties caused by the neighboring channel were <1.0 dB with and without the 20-km long feeder fiber. Thus, in the proposed UD-WDM PON, the total crosstalk penalty would be <2 dB since the crosstalk arose mostly from the immediately neighboring two channels. This figure also showed that the power penalty caused by the 20-km long transmission was 1.2 dB. We attributed most of this penalty to the Rayleigh backscattered upstream signal (as it was modulated again by the RSOA and interfered with the original upstream signal) [25]. The power penalty caused by using the comb generator for the seed light instead of a bank of tunable lasers was measured to be <0.5 dB. In the proposed UD-WDM PON, the receiver sensitivities (@ BER = 10^{-3}) of the 12.5-GHz spaced, 12.5-Gb/s upstream QPSK signals were measured to be -31.3 dBm.

In this demonstration, the power budget of the upstream signals was limited primarily by the power requirement of the seed light incident on the RSOA. For example, the RSOA used in this experiment required the seed power to be larger than -12 dBm. On the other hand, the optical power of each comb line (which was used as the seed light) should be less than 3 dBm to avoid the deleterious effects of FWM. Thus, in the proposed UD-WDM PON, the power budget for the upstream transmission was estimated to be 15 dB. Considering the insertion losses of an AWG (5 dB), two wavelength-division multiplexers (2×1 dB), 20-km long feeder fiber (0.25 dB/km \times 20 km), and an FR (0.5 dB), we could still secure the power margin of 2.5 dB. To further improve this power margin, it would be necessary to utilize the RSOAs with a low input saturation power.

5. Summary

We have proposed and demonstrated a practical 12.5-Gb/s, 12.5-GHz spaced UD-WDM PON. For the cost-effectiveness, we implemented the downstream links by using EMLs modulated in the 4PAM format and PIN receivers, and the upstream links by using directly modulated RSOAs in the QPSK format and inexpensive self-homodyne receivers developed for the use in the access networks. To further enhance its cost-effectiveness, we also utilized an optical frequency comb generator, instead of a large number of wavelength-selected lasers, to provide the seed light for these colorless RSOAs. For the proper operation of these downstream and upstream links in the presence of the crosstalk arising from the closely spaced neighboring channels and the ISI caused by the narrow passband of the cascaded AWGs, we optimized the ER of EMLs and the bias and modulation currents of RSOAs. As a result, we could achieve the error-free transmission of these 12.5-Gb/s signals, spaced at 12.5-GHz, even after the 20-km long SSMF transmission. The crosstalk-induced penalties were negligible (<0.1 dB) for the downstream signals and <1 dB for the upstream signals. The ISI-induced penalties were measured to be less than 1.1 dB and 4.2 dB for the downstream and upstream signals, respectively.

Acknowledgment

This work was partially supported by the National Research Foundation of Korea (NRF) grant funded by the Korea government (MSIP) (2012R1A2A1A01010082).